Length scales and dissipation of fine eddies in a mixing layer

By Y. Zohar[1], R. D. Moser[2], J. C. Buell[3] AND C. M. Ho[1]

It has been shown that small scale turbulence is produced by the interaction of the merging spanwise structures (rollers) and the streamwise vortices (ribs) (Huang & Ho 1990, Moser & Rogers 1990). In this study, we examine the dissipation rate of the three-dimensional kinetic energy and the length scales associated with the dissipation rate in a temporally-evolving mixing layer.

1. Introduction

It has been recognized that entrainment of fluids from the two streams into the shear region of a mixing layer is controlled by the unsteady evolution of the large coherent structures. The fine-scale mixing of the two fluids is accomplished by the random small eddies which produce a larger mixing interface area (Ho & Huerre 1984). This paper presents some properties of these fine-scale eddies.

The small-scale transition characterized by the sudden increase of the roll-off exponent of the energy spectrum near the first vortex merging was reported by Huang & Ho (1990). They used the Peak-Valley-Counting (PVC) technique to directly detect the small-scale velocity fluctuations and found that the small-scale activity was initially concentrated in regions corresponding to the cores of the merging rollers and in the plane containing the streamwise vortices. Hence, they suggested that the interaction between these two deterministic structures during vortex merging leads to the production of small eddies. Zohar & Ho (1990) then further developed the PVC technique to gain more physical insight into the small-scale eddies. They found that the most probable length scale of the fine eddies is equal to the scale of maximum dissipation, suggesting that the structures detected by the PVC technique are responsible for most of the dissipation of kinetic energy. Furthermore, the maximum strain rate associated with the small eddies was found to scale with the global strain rate associated with the coherent structures.

In the experiment, the PVC technique was applied to the streamwise velocity signal recorded by a hot-wire at a single point in the flow field. The length scale was obtained by converting time into length through the Taylor hypothesis. In the flow, the eddies are distributed in space, so the length scale determined from a single point is only a component of the averaged distance between eddies. However, in a numerically simulated mixing layer, the entire velocity field is readily available.

1 University of Southern California
2 NASA Ames Research Center
3 Center for Turbulence Research

It is then possible to extend the PVC technique to a 2-D x–z surface (x is the streamwise and z is the spanwise direction) instead of the 1-D time (or pseudo-x) trace. Furthermore, the PVC technique can be applied to velocity components other than the streamwise, and even to other quantities such as vorticity.

The dissipation of turbulent energy is mainly due to the effect of viscosity on small scales. In experiments, due to the limitation of having only a few sampling points in space, the study of dissipation has concentrated on time-averaged quantities. However, using numerical simulation data, the spatial distribution of the viscous dissipation can be examined.

Several numerically simulated time-evolving mixing layers are available. For the current study we have selected a simulation which undergoes two pairings. By the second pairing, the layer has completed the transition to small-scale turbulence. This simulation is described by Moser & Rogers (1990). The numerical results reported below were all taken from this simulation at the time of the second pairing.

2. The peak-valley-counting (PVC) technique

The study of fine-scale eddies in the past was restricted to statistical analyses, however these techniques do not provide the phase and amplitude information of the small eddies. Huang & Ho (1990) and Hsiao (1985) started to develop a method of registering both the instant and the magnitude of an event whenever the velocity signal exhibits a peak or a valley (PVC technique). Although the concept is simple, it is difficult to distinguish between the actual small eddies and instrument or numerical noise. Recently, Zohar (1990) has significantly alleviated this problem by applying several conditional criteria.

The PVC technique locates the extrema of the velocity fluctuations induced by the small eddies. The interval between a peak-valley pair provides a length scale for the event. Since the velocity difference between the peak and the valley is also registered, the average strain rate associated with that event can be obtained as well.

In the current work, the PVC technique based on the 1-D time trace of velocity fluctuations has been extended to a 2-D plane of velocity data taken from a computational mixing layer. The stationary points of the velocity field on a given surface, (i.e. extrema and saddle points) where both directional derivatives vanish ($\partial/\partial x = \partial/\partial z = 0$) are first identified. Noise effects are minimized by eliminating extraneous stationary points using criteria similar to those used by Zohar (1990). The stationary points are then connected together in an unstructured mesh using the greedy algorithm. The length scales and strain rates can then be calculated from the probability distribution function (pdf) of the distance between stationary points and the velocity difference between these points.

3. Spatial distributions of small-scale turbulence

The spatial distribution of the velocity fluctuations associated with small-scale turbulence is represented by the stationary points determined from the 2-D PVC method. The technique has been applied to all three velocity components. It is

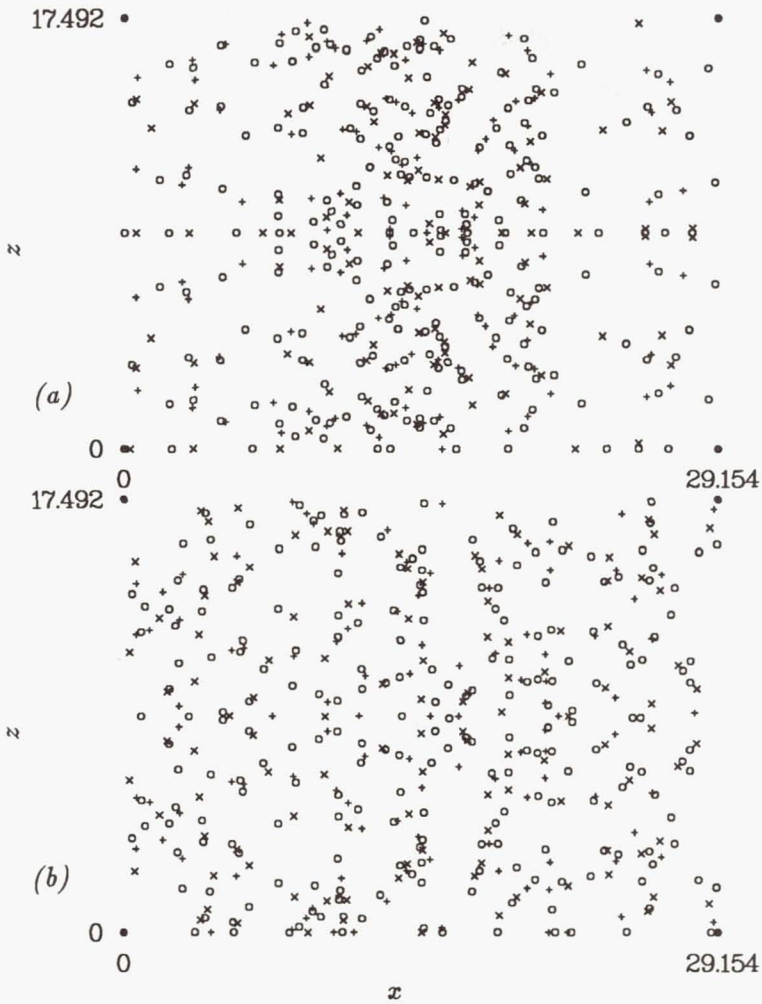

FIGURE 1. Location of two-dimensional stationary points of *(a)* u, and *(b)* v in the x–z plane at $y = 0$. The stationary points are: $\times$, minima; $\circ$, saddles; and $+$, maxima. The spanwise roller is centered in the x domain.

very interesting to note that the patterns of the stationary points in each of the three velocity components are quite different. In figure 1, the streamwise velocity fluctuations, u, show higher concentration of fine eddies along the roller core than in the braid region. Similarly, Zohar & Ho (1990) found in their experiment that the small-scale activity in the roller core is about twice that in the braid region. However, the transverse velocity fluctuations, v, have a uniform distribution in the x–z plane (figure 1*b*). This finding is somewhat surprising and is not yet understood. Farge *et al.* (1990) applied the wavelet analysis to the same velocity field. They also observed that the energy content of the transverse velocity fluctuations at high wavenumbers is evenly distributed. The spanwise velocity fluctuations, w, have a

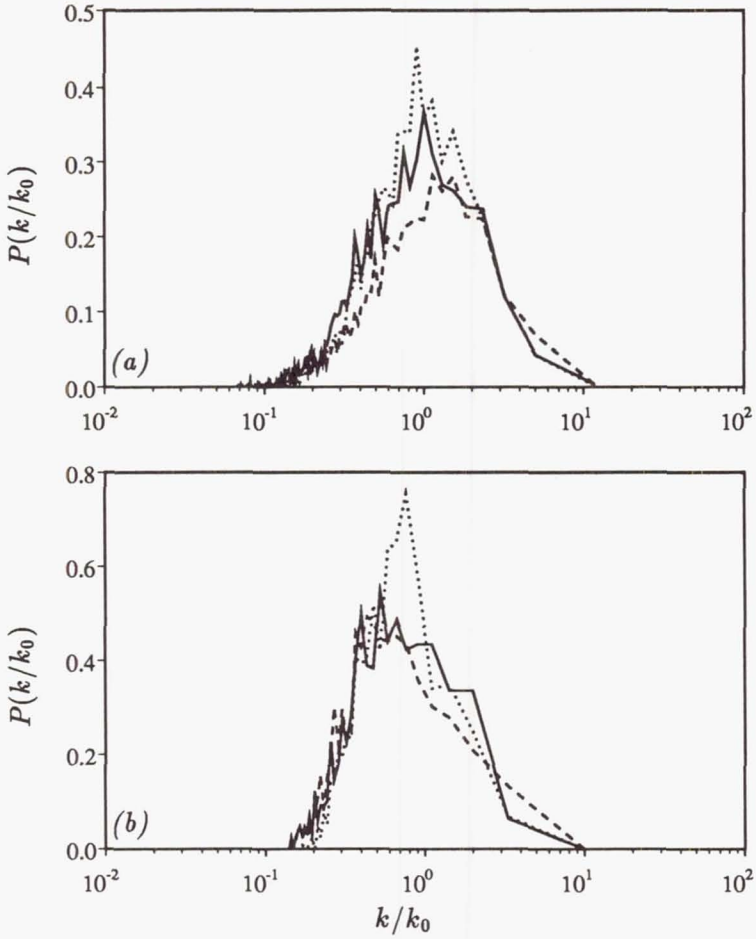

FIGURE 2. Probability density of the wavenumbers $k_i = 2\pi/d_i$, where the d_i are the separations between stationary points in the *(a)* one-dimensional and *(b)* two-dimensional PVC technique based on: ——— , streamwise velocity u; ---- , cross-stream velocity v; and ····· , spanwise velocity w.

stationary point distribution pattern similar to that of the streamwise fluctuating velocity, but the number of stationary points is about 50% higher than for the streamwise component.

4. Length scales of fine eddies

4.1. Length scales of velocity fluctuations

The distance, d_i, between a peak-valley pair yields a measure for the size of the fine eddies. At the extremum, in the 1-D PVC, the velocity derivative is zero. Therefore, d_i is just the distance between zero crossings of the first velocity derivative. The pdf of the corresponding wavenumbers, $k_i = 2\pi/d_i$, is constructed for the 3 velocity components; u, v and w as shown in figure 2*a*. The pdf curves have a

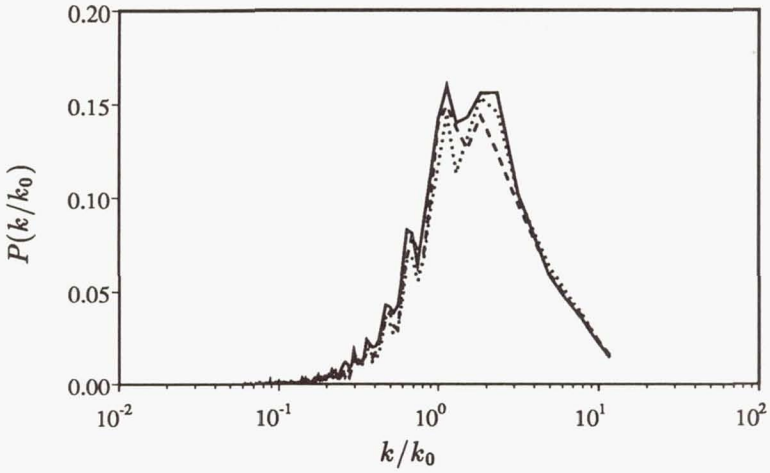

FIGURE 3. Probability density of the wavenumbers $k_i = 2\pi/d_i$, where the d_i are the separations between stationary points in the one-dimensional PVC technique based on: ——— , streamwise vorticity ω_x; ---- , cross-stream vorticity ω_y; and ····· , spanwise vorticity ω_z.

clear sharp peak. The wavelength at the peaks, denoted as $L_s = 2\pi/k_s$, is used as the length scale to characterize the size of the fine eddies. Based on the numerical data, the pdf curves of the three velocity components peak at $k_s/k_0 \simeq 1$, where $k_0 = 2\pi/\delta_0$ and δ_0 is the initial vorticity thickness of the mixing layer. Experimentally, the value of this ratio, k_s/k_0, was found to be about 5. This difference could be due to the difference in initial Reynolds number between the experiment and simulation. In the numerical simulation, $Re = \Delta U \delta_0/\nu = 500$, but $Re = 2000$ in the experiment. It is expected that the fine eddies should have a smaller length scale in the flow with the higher Reynolds number.

Next, the 2-D PVC technique is applied to the velocity components in a horizontal, x–z plane. The pdf curves of wavenumbers based on the length of the line segments connecting the stationary points are similar to the 1-D results, i.e. there is a clear peak as shown in figure 2*a*. The wavenumber at the peak is smaller than the value for the 1-D case, $k_s/k_0 \simeq 0.7$. The d_i measured by the 1-D technique are projections of the d_i measured by the 2-D technique. Therefore, the d_i obtained from the 1-D PVC are expected to be shorter than those for the 2-D PVC, at least in the case of 2-D isotropy.

4.2. Length scales for vorticity fluctuations

Both the 1-D and the 2-D PVC techniques can be applied to other fluctuating quantities. Vorticity is obviously an interesting quantity to be examined. Due to noise problems in the vorticity signal, only the results of the 1-D PVC technique are presented (figure 3). The peak of the pdf curves of the vorticity peak-valley wavenumbers is at $k_s/k_0 \simeq 1.25$. This value is larger than the peak value of the velocity fluctuations. Vorticity is derived from derivatives of velocity fluctuations.

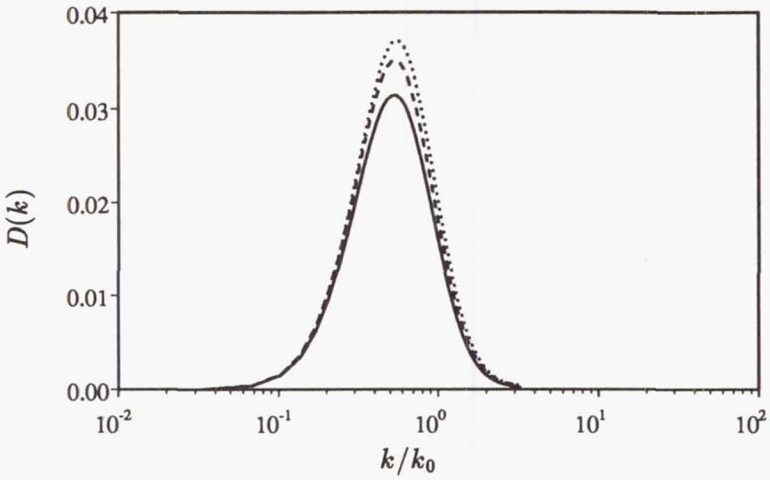

FIGURE 4. Dissipation spectrum $D(k)$ estimated from equation (2), based on the velocity spectrum at: ——— , $y = 0$; - - - - , $y = 1$; and ····· , $y = 2$.

Spatial differentiation emphasizes the high wavenumber end of the spectrum and therefore the vorticity length scale is shorter than the velocity length scale. Moreover, velocity fluctuations are detected in the potential flow regions as well, where the vorticity fluctuations vanish. These potential velocity fluctuations are found to have longer wavelengths compared to the rotational fluctuations. Nevertheless, the most probable length scale of the fluctuating vorticity and the fluctuating velocity components are of the same order of magnitude in this low-Reynolds-number flow.

4.3. A new dissipative scale

The physical significance of the length scale based on the PVC technique has been pointed out by Zohar & Ho (1990). L_s corresponds to the wavelength at the peak of the dissipation spectrum, $D(k)$. In order to verify this for other velocity components the dissipation spectrum should be estimated. First, the 3-D energy spectrum, $E(k)$, is calculated from the 1-D energy spectrum of the streamwise velocity, $F_{uu}(k)$, by using the following isotropic relationship,

$$E(k) = k^3 \frac{d}{dk}\left[\frac{1}{k}\frac{d}{dk}F_{uu}(k)\right] \tag{1}$$

Then, the dissipation spectrum can be obtained from the 3-D energy spectrum as follows,

$$D(k) = k^2 E(k) \tag{2}$$

The peak of the dissipation spectrum, shown in figure 4, appears at $k_s/k_0 \simeq 0.7$. Indeed, it is equal to the most probable length scale obtained from the 2-D PVC technique. This suggests that the small-scale eddies detected by the 2-D PVC scheme dissipate most of the kinetic energy. A similar correspondence between k_s and the peak in the dissipation spectrum was found by Zohar (1990) in his 1-D PVC experiment.

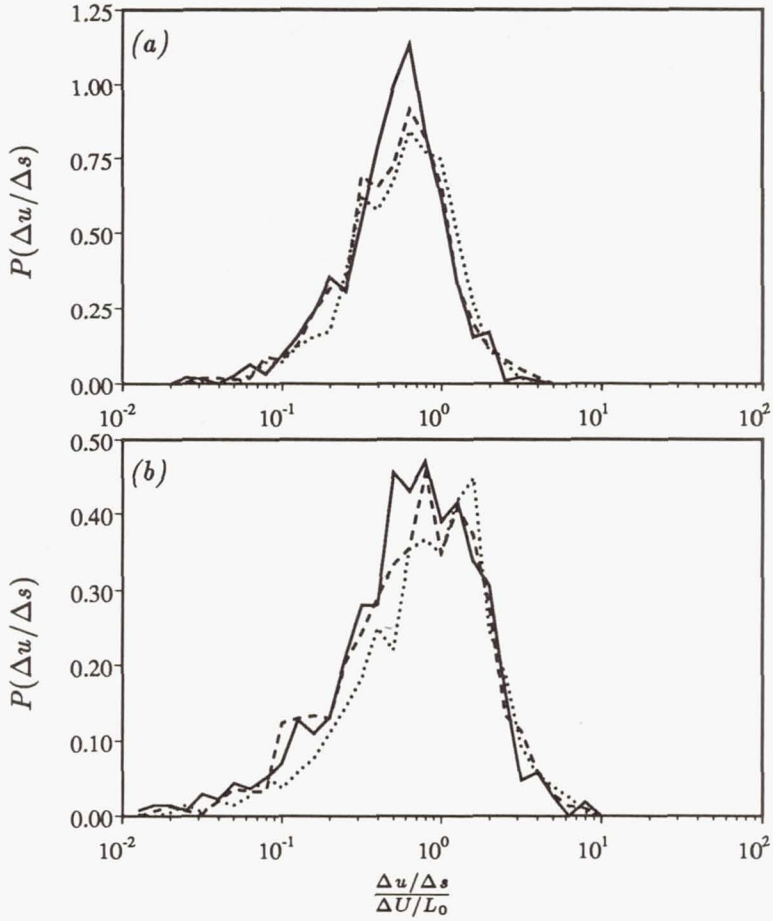

FIGURE 5. Probability density of the average small-scale strain rate $\Delta u/\Delta s$ obtained from the *(a)*, one-dimensional and *(b)*, two-dimensional PVC technique based on the streamwise velocity at —— $y = 0$, ---- $y = 1$ and ····· $y = 2$.

5. Strain rates

The PVC technique enables one to estimate the average strain rate associated with the small eddies. This estimate is obtained by dividing the velocity difference between adjacent extrema or stationary points, Δu, by the length separating them, Δx in a 1-D trace or Δs in a 2-D plane. Then, the collection of all values of $|\Delta u/\Delta x|$ or $|\Delta u/\Delta s|$ can be used to construct a histogram for the local strain rate. These strain rates are normalized by the total velocity difference across the mixing layer, ΔU, and the initial instability wavelength, L_0. Figure 5*a* shows the pdf of the strain rate based on 1-D traces of the streamwise velocity, where the maximum occurs at a normalized strain rate of 0.6. The pdf based on the 2-D plane of the streamwise velocity peaks around 1, as shown in figure 5*b*. This value agrees with the experimental data based on the 1-D PVC technique.

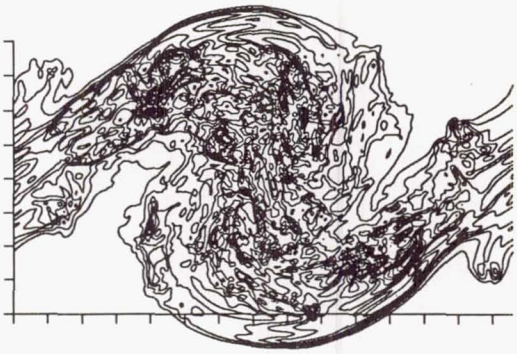

FIGURE 6. Spanwise average of the 3-dimensional strain contraction $2S_{ij}S_{ij} = \epsilon/\nu$. The contour increment is 0.5 and the highest contour level is 8.

6. Spatial distribution of dissipation

Turbulent flow is three dimensional in nature. In order to investigate the dissipation-rate of 3-D kinetic energy, the velocity is first averaged along the spanwise direction to obtain the 2-D averaged velocity field. The 3-D velocity field was obtained by subtracting the 2-D averaged velocity from the total velocity. Dissipation can then be calculated from the resultant 3-D velocity. The instantaneous local dissipation of turbulent kinetic energy can be written $\epsilon = 2\nu S_{ij}S_{ij}$, where S_{ij} is the strain tensor. The spanwise average of ϵ/ν (or strain contraction) is shown in figure 6. The strain contraction (ϵ/ν) in the x–y plane between the rib vortices and through the rib vortices is shown in figure 7. Also shown is the enstrophy ($\omega_i\omega_i$) in the same planes. As would be expected from the spatial location of the small scales, the dissipation occurs largely in the roller. There is however some dissipation associated with the braid-region ribs in the rib plane. The enstrophy contours show that the enstrophy is much more intermittent than the dissipation. Nearly all the enstrophy hot-spots are associated with significant dissipation, though there is also significant dissipation in essentially irrotational regions. It is interesting to note that the volume integral of $S_{ij}S_{ij}$ over the domain is the same as that of the enstrophy. Thus, the smaller regions of support for the enstrophy imply (as is visible in figure 7), that the peak magnitudes are much larger than for ϵ/ν.

7. Conclusions

The PVC signal processing technique is indeed a useful tool for studying small-scale turbulence from a new perspective. The technique has been extended to a two-dimensional velocity field. The data from the 2-D PVC technique are slightly different from that of the 1-D PVC technique. The results derived from the numerical simulations confirm the experimental findings; the most probable length scale of the small-scale eddies is equal to the scale of maximum dissipation and the local strain rates associated with the small-scale activity are comparable to the global strain rate, $\Delta U/L_0$.

The dissipation was seen to occur mostly in the mixing layer rollers, consistent

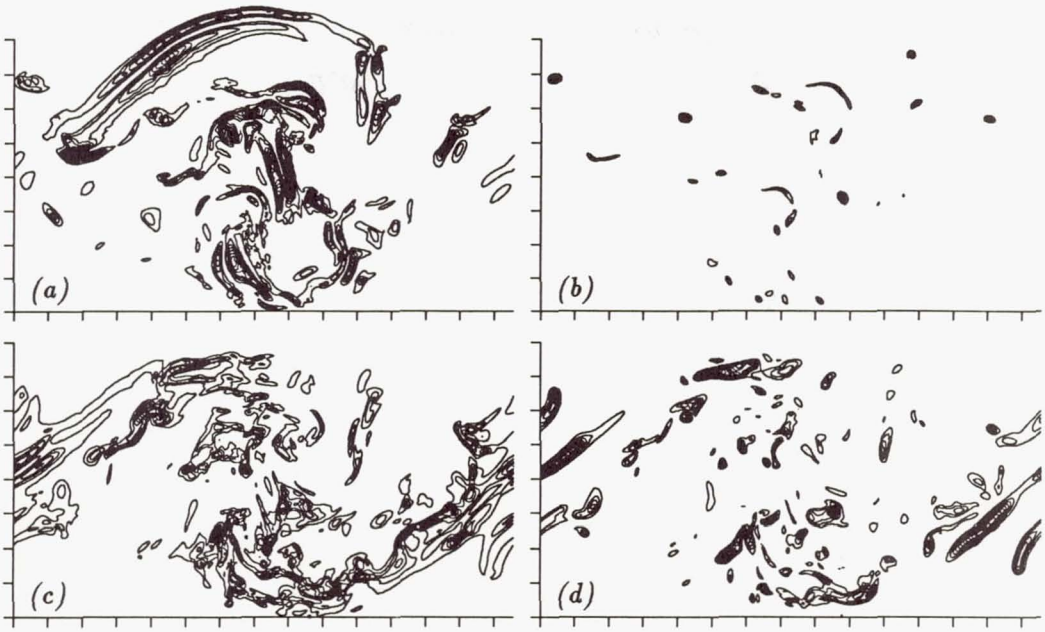

FIGURE 7. The 3-dimensional strain contraction $2S_{ij}S_{ij} = \epsilon/\nu$ (*(a)* and *(c)*) and the enstrophy $\omega_i\omega_i$ (*(b)* and *(d)*) in an x–y plane between the rib vortices (*(a)* and *(b)*) and through the rib vortices (*(c)* and *(d)*). The contour increment in 2.5. The spanwise roller is centered in the domain.

with the observation that the small-scale eddies are located there. The enstrophy is much more intermittent than the dissipation. There were many dissipating regions which were essentially irrotational.

REFERENCES

FARGE, M., GUEZENNEC, Y., HO, C. M. & MENEVEAU, C. 1990 Continuous wavelet analysis of coherent structures. *In this volume.*

HO, C. M. & HUERRE, P. 1984 Perturbed free shear layers. *Ann. Rev. Fluid Mech.* **16**, 365-424.

HSIAO, F. B. 1985 Small scale transition and preferred mode in an initially laminar plane jet. *Ph.D. thesis,*Univ. South. Calif., Los Angeles.

HUANG, L. S. & HO, C. M. 1990 Small scale transition in a plane mixing layer. *J. Fluid Mech.* **210**, 475-500.

MOSER, R. D. & ROGERS, M. M. 1990 Mixing transition and the cascade to small scales in a plane mixing layer. *Proc. IUTAM Symposium on Stirring and Mixing.* La Jolla, Ca., 20-24 August, 1990.

ZOHAR, Y. 1990 Fine scale mixing in a plane mixing layer. *Ph.D. thesis,* Univ. South. Calif., Los Angeles.

ZOHAR, Y. & HO, C. M. 1990 Fine-eddy production and control in a mixing layer. *In preparation.*